Laser spectroscopy of NiI: Ground and low-lying electronic states

W. S. Tam, J. W.-H. Leung, Shui-Ming Hu,[a] and A. S.-C. Cheung[b]
Department of Chemistry, The University of Hong Kong, Pokfulam Road, Hong Kong

(Received 5 September 2003; accepted 23 September 2003)

High-resolution laser-induced fluorescence spectrum of a jet-cooled NiI molecule has been recorded in the near infrared and visible regions. The NiI molecule was produced by reacting laser-ablated nickel atom and methyl iodide (CH_3I). Three electronic states have been identified that include the $X\,^2\Delta_{5/2}$ and two low-lying [13.9] $^2\Pi_{3/2}$ and [14.6] $^2\Delta_{5/2}$ excited states. Molecular transition bands (v',0) of the [13.9] $^2\Pi_{3/2}-X\,^2\Delta_{5/2}$ system with $v'=0$, 4–9, and the (v',0) bands of the [14.6] $^2\Delta_{5/2}-X\,^2\Delta_{5/2}$ system with $v'=0-6$ were observed and analyzed. Spectra of isotopic molecules confirmed the assignment of vibrational quantum number of the observed bands. Least squares fit of rotational transition lines yielded accurate molecular constants for the states studied. The bond length r_0 measured for the $X\,^2\Delta_{5/2}$ is 2.3479 Å and the equilibrium bond length, r_e, for the [13.9] $^2\Pi_{3/2}$ and [14.6] $^2\Delta_{5/2}$ are, respectively, 2.4834 and 2.5081 Å. With the use of a molecular orbital energy level diagram, we have examined the electronic configurations that give rise to the $X\,^2\Pi_{3/2}$ ground state for NiF, NiCl, and NiBr, but the $X\,^2\Delta_{5/2}$ state for NiI. This work represents the first spectroscopic study of the NiI molecule. © *2003 American Institute of Physics.* [DOI: 10.1063/1.1625921]

I. INTRODUCTION

Transition metal monohalides are important model systems for understanding the role of the *d* electrons in chemical bonding.[1] Spectroscopic studies of these monohalides yield useful information on *d* orbital occupation in chemical bonds, and it is interesting to compare in detail the spectroscopic properties of various monohalides to examine the effects of the halogens as a ligand to the transition metal *d* orbitals. Among the first transition metal period, there has been considerable interest in the spectroscopic properties of nickel monohalides in recent years.[2–24] Work includes study of the ground and excited states using high resolution Fourier transform (FT) spectroscopy, FT microwave spectroscopy, and laser-induced fluorescence spectroscopy. For NiF[2–12] and NiCl,[12–19] good knowledge of electronic structure of the ground and excited states has been obtained through years of hard work of many workers, however, for the latter two nickel monohalides, namely, NiBr and NiI, only limited spectroscopic information is available. Recently Leung *et al.*[24] using high resolution laser spectroscopy, identified unambiguously the ground and three low-lying electronic states for NiBr, but, up until the present moment, nothing is known for NiI.

In this paper, we report rotationally resolved near-infrared and visible spectroscopic studies of the ground and low-lying electronic states of NiI using the technique of laser vaporization/reaction with free jet expansion and laser-induced fluorescence (LIF) spectroscopy. Two electronic transitions: the [13.9] $^2\Pi_{3/2}-X\,^2\Delta_{5/2}$ system and the [14.6] $^2\Delta_{5/2}-X\,^2\Delta_{5/2}$ system have been recorded and analyzed. Spectra of isotopic molecules: ^{58}NiI and ^{60}NiI were observed and analyzed. Line positions measured for both isotopes were fit to retrieve vibrational and rotational constants for $X\,^2\Delta_{5/2}$, [13.9] $^2\Pi_{3/2}$ and [14.6] $^2\Delta_{5/2}$ states. In addition, with the use of a molecular orbital energy level diagram, we have examined the electronic configurations that give rise to the $X\,^2\Pi_{3/2}$ ground state for NiF, NiCl, and NiBr, but the $X\,^2\Delta_{5/2}$ state for NiI.

II. EXPERIMENTAL DETAILS

NiI molecule was produced by the reaction of laser-ablated nickel atom with methyl iodide (CH_3I) under supersonic free jet conditions, and NiI spectra were recorded using laser-induced fluorescence spectroscopy. Experimental apparatus used in this experiment, detailed procedures for generating transition metal containing molecules and recording their LIF spectra have been discussed in our earlier publication,[25,26] only a brief description of the experimental conditions is given here. A laser pulse of 532 nm, 9–10 mJ from a Nd:YAG laser was focused on the surface of a nickel metal rod to generate nickel atoms. A pulsed valve, with an appropriate delay, released gas mixture of 3% CH_3I in argon to react with the nickel atoms. The operating cycle of the Nd:YAG laser-pulsed valve system was 10 Hz. The backing pressure at the pulsed valve was set to 5 atm. The jet-cooled NiI molecule was excited by an argon ion pumped ring dye laser operating with DCM and R6G dyes in the visible region and a ring Ti:sapphire laser with short-wavelength (SW) optics in the near-infrared region. The laser-induced fluorescence signal was collected by a lens system and detected by a photomultiplier tube (PMT). The PMT signal was fed into a boxcar integrator for averaging. The width of the molecular

[a]Permanent address: Laboratory of Bond Selective Chemistry, University of Science and Technology of China, Hefei, Anhui 230026, People's Republic of China.
[b]Author to whom correspondence should be addressed; fax: (852)2857-1586; electronic mail: hrsccsc@hku.hk

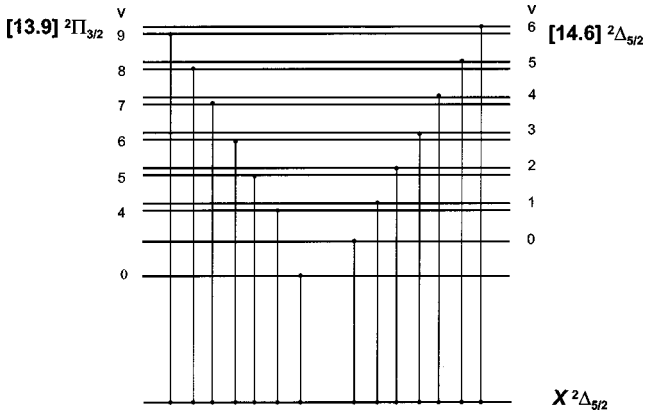

FIG. 1. Vibronic transitions observed and analyzed in this work.

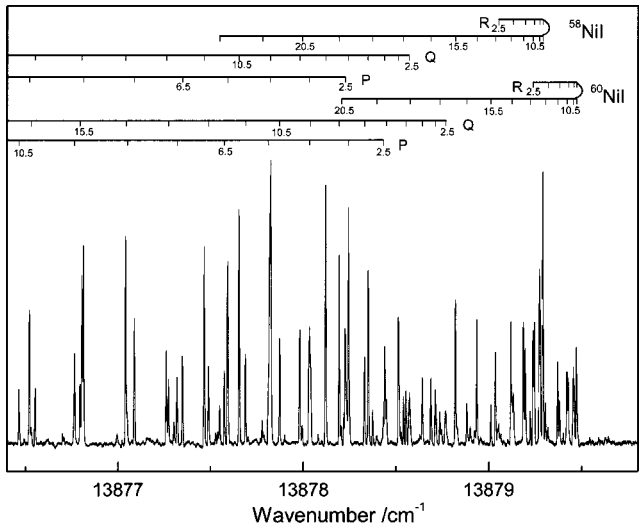

FIG. 2. The (0, 0) band of the [13.9] $^2\Pi_{3/2}-X\,^2\Delta_{5/2}$ transition of NiI.

transition lines measured was about 250 MHz. The wavelength output of both the dye and the Ti: sapphire lasers was measured by a wavemeter with a repetition rate of 1 Hz and an accuracy of 1 part in 10^7. The absolute wavelength calibration of the wavemeter was checked against I_2 absorption lines, which were accurate to about ± 0.002 cm^{-1} in the visible and near-IR regions.[27] Hundreds of scans were made and connected together by a computer program using the wavemeter readings.

III. RESULTS AND DISCUSSION

A. General features

The laser-induced fluorescence spectrum of NiI in the visible region between 588 and 720 nm has been observed and analyzed. Molecular transition bands are generally easy to identify because of the small B value (0.065 cm^{-1}) and reasonable large vibrational separations (230 cm^{-1}). Two transition systems: [13.9] $^2\Pi_{3/2}-X\,^2\Delta_{5/2}$ and [14.6] $^2\Delta_{5/2}-X\,^2\Delta_{5/2}$ were observed and analyzed. Our spectra showed that the [13.9] $^2\Pi_{3/2}-X\,^2\Delta_{5/2}$ system is slightly weaker than the [14.6] $^2\Delta_{5/2}-X\,^2\Delta_{5/2}$ system. Figure 1 depicts the vibronic transition bands studied in this work.

B. [13.9] $^2\Pi_{3/2}-X\,^2\Delta_{5/2}$ system

Our initial survey spectrum indicated that the molecular transition bands, obtained using the DCM dye, were high in vibrational numbering because of large isotopic shifts. Six band heads appear at 14 803.6, 15 030.7, 15 256.3, 15 480.3, 15 702.6, and 15 923.4 cm^{-1} were assigned as the $(v,0)$ bands with $v=4-9$. Based on the vibrational separations of the observed vibronic bands and also the isotopic shifts, the vibrational numbering of the upper state was assigned unambiguously. Further to the assignment of the $(v,0)$ bands with $v=4-9$, we made use of the vibrational information to predict the origin of the other bands with lower vibrational quantum number. Using our Ti:sapphire laser with short wave (SW) optics, the (0,0) band head was observed at 13 879.3 cm^{-1}. Due to the limitation in laser coverage, we could not record the $(v,0)$ band with $v=1-3$. The observed band consists of resolved P, Q, and R branches. Line assignments were simple because the first line of each branch was identified. Figure 2 shows the band head region of the (0, 0) band, the R branch head of the ^{58}NiI and ^{60}NiI lie very closed to each other. The P, Q, and R branches have a first line with $J=2.5$, which established the upper and lower substates, have Ω' and Ω'' values of 1.5 and 2.5, respectively. It is easily noticed that the Q and P branches are stronger in intensity than the R branch, which is consistent with a transition of $\Delta\Lambda=-1$. We have assigned the transition as the [13.9] $^2\Pi_{3/2}-X\ ^2\Delta_{5/2}$ system. Since our spectrum was recorded at a relatively low temperature, only low J lines were observed ($J\leqslant 30.5$), no Λ-type doubling was detected. The observed line positions were fit to a standard formula:

$$\nu = T_0 + B'J'(J'+1) - D'[J'(J'+1)]^2 - \{B''J''(J''+1) - D''[J''(J''+1)]^2\}, \quad (1)$$

where the usual meaning of $'$ and $''$ are, respectively, for upper and lower states. In our analysis, a band-by-band least squares fit to the line positions was initially performed and subsequently all the available line positions of each isotopic molecule were merged together in the final fit. The centrifugal correction terms for both the upper and lower states were set to the value derived from the Kratzer relation. Our results are listed in Table I.

C. [14.6] $^2\Delta_{5/2}-X\,^2\Delta_{5/2}$ system

Seven vibronic transition $(v,0)$ bands with $v=0-6$ of this system was observed. Each of these bands consists of resolved P, Q, and R branches. Figure 3 shows the band head region of the (1, 0) band of this system. The first line of each P, Q, and R branches are, respectively, with $J=3.5$, 2.5, and 2.5, which indicated that $\Omega'=\Omega''=2.5$ for both upper and lower states. The intensity of the P and R branches is higher than the Q branch, which agrees well with a $\Delta\Omega=0$ and $\Delta\Lambda=0$ transition. The observed transition has been assigned as the [14.6] $^2\Delta_{5/2}-X\,^2\Delta_{5/2}$ system. We have noticed that the $v=6$ band observed in this system has a sizable linewidth at low J values. Since ^{58}Ni and ^{60}Ni have no nuclear spin, such an increase in the linewidth is caused by the magnetic hyperfine interaction of the magnetic moment of un-

TABLE I. Derived constants for the [13.9] $^2\Pi_{3/2}-X\,^2\Delta_{5/2}$ transition of both ^{58}NiI and ^{60}NiI (cm^{-1}).[a]

Molecule	v	[13.9] $^2\Pi_{3/2}$ T_v	[13.9] $^2\Pi_{3/2}$ B_v	$X\,^2\Delta_{5/2}$ B_0
^{58}NiI	0	13 878.6414(2)	0.068 686(1)	0.076 857(2)
	4	14 803.0374(2)	0.067 553(1)	
	5	15 030.2211(2)	0.067 266(1)	
	6	15 255.8132(3)	0.066 979(1)	
	7	15 479.7988(3)	0.066 683(1)	
	8	15 702.1613(2)	0.066 393(1)	
	9	15 922.8820(4)	0.066 099(1)	
^{60}NiI	0	13 878.8380(3)	0.067 142(1)	0.075 129(3)
	5	15 017.4500(2)	0.065 766(1)	
	6	15 240.5603(2)	0.065 490(1)	

[a]Errors in parentheses are one standard deviation in the units of the last significant figure quoted.

TABLE II. Molecular constants for the [14.6] $^2\Delta_{5/2}-X\,^2\Delta_{5/2}$ transition of both ^{58}NiI and ^{60}NiI (cm^{-1}).[a]

Molecule	v	[14.6] $^2\Delta_{5/2}$ T_v	[14.6] $^2\Delta_{5/2}$ B_v	$X\,^2\Delta_{5/2}$ B_0
^{58}NiI	0	14 583.7363(5)	0.067 368(3)	0.076 857(2)
	1	14 812.5118(3)	0.067 089(2)	
	2	15 039.5623(3)	0.068 180(2)	
	3	15 264.8665(3)	0.066 545(2)	
	4	15 488.3801(3)	0.066 270(2)	
	5	15 710.1048(3)	0.066 002(2)	
	6	15 930.1456(3)	0.065 747(2)	
^{60}NiI	1	14 810.1346(3)	0.065 583(3)	0.075 129(3)
	2	15 034.6193(3)	0.065 316(3)	
	3	15 257.3935(3)	0.065 053(3)	
	4	15 478.4216(3)	0.064 789(3)	
	5	15 697.7214(3)	0.064 529(3)	
	6	15 915.4628(3)	0.064 303(3)	

[a]Errors in parentheses are one standard deviation in the units of the last significant figure quoted.

paired electrons with the magnetic moment of the iodine nucleus with $I=\frac{5}{2}$, and may possibly also come from the electric quadrupole interaction of the iodine nucleus spin. Work is currently in progress to study the details of the hyperfine structure. We have performed a least squares fit to the line positions of the observed bands using the expression in Eq. (1). The results are listed in Table II. A list of line positions of the two isotopes for the vibronic bands observed for both [13.9] $^2\Pi_{3/2}-X\,^2\Delta_{5/2}$ and [14.6] $^2\Delta_{5/2}-X\,^2\Delta_{5/2}$ systems of NiI is available from EPAPS.[28] The root-mean-squares (rms) error of the merged least squares fit was 0.0018 cm^{-1}. Molecular constants for the $X\,^2\Delta_{5/2}$, [13.9] $^2\Pi_{3/2}$, and [14.6] $^2\Delta_{5/2}$ states are reported for the first time. Equilibrium molecular constants for [13.6] $^2\Pi_{3/2}$ and [14.6] $^2\Delta_{5/2}$ states for NiI are listed in Table III.

D. Isotopic relationship between ^{58}NiI and ^{60}NiI

The vibrational quantum number assignment of the vibronic bands observed was confirmed by examining the isotopic relationship of the observed bands. The molecular parameter of isotopic molecules are approximately related by different powers of the mass dependence $\rho=(\mu/\mu_i)^{1/2}$, where μ and μ_i are the, respectively, reduced mass of ^{58}NiI and ^{60}NiI.[29] Table III shows a comparison of the calculated and observed equilibrium molecular parameters. The agreement of these parameters is excellent.

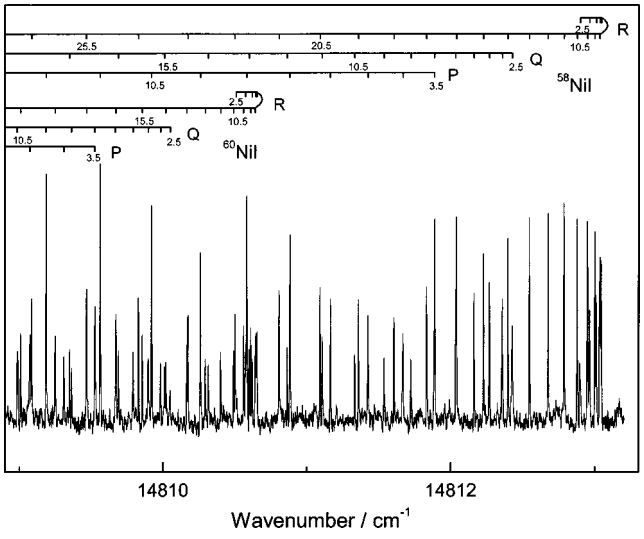

FIG. 3. The (1, 0) band of the [14.6] $^2\Delta_{5/2}-X\,^2\Delta_{5/2}$ transition of NiI.

E. Electronic configurations and ground state of nickel monohalides

From the available spectroscopic information, the effect of a halogen as a ligand to split the nickel d orbitals can be examined. Figure 4 presents qualitatively the relative energy of the molecular orbitals (MOs) formed from Ni and the halogens. Since the halogen atom has no valence orbital with δ symmetry, the 1δ MO is essentially unaffected by the halogen atom, therefore, the MOs are arranged so that the 1δ MO of the monohalides is placed at the same energy in the figure. The construction of the molecular orbital energy level diagram depends on the relative energy of the $3d$, $4s$, and $4p$ orbitals of the Ni atom and the p orbitals of the halogen atom. The ionization potential (IP) of the Ni and halogen

TABLE III. Equilibrium molecular constants for the [13.9] $^2\Pi_{3/2}$ and the [14.6] $^2\Delta_{5/2}$ states of ^{58}NiI and ^{60}NiI (cm^{-1}).

State	Parameter	^{58}NiI	^{60}NiI[a] Obs.	^{60}NiI[a] Calc.[b]
[13.9] $^2\Pi_{3/2}$	T_e	13 761.28(4)	13 762.86	–
	ω_e	235.09(2)	232.34	232.34
	$\omega_e x_e$	0.794(2)	0.769	0.767
	B_e	0.068 840(7)	0.067 280	0.067 270
	α_e	0.000 288(1)	0.000 275	0.000 278
[14.6] $^2\Delta_{5/2}$	T_e	14 468.67(2)	14 468.67(2)	–
	ω_e	230.56(1)	227.86(6)	227.91
	$\omega_e x_e$	0.879(2)	0.850(7)	0.086
	B_e	0.067 497(6)	0.065 960(1)	0.065 950
	α_e	0.000 271(1)	0.000 257(3)	0.000 261

[a]Uncertainty for the parameter could not be obtained from the least square fit.

[b]Molecular constants were calculated using isotopic relationships and the values from ^{58}NiI.

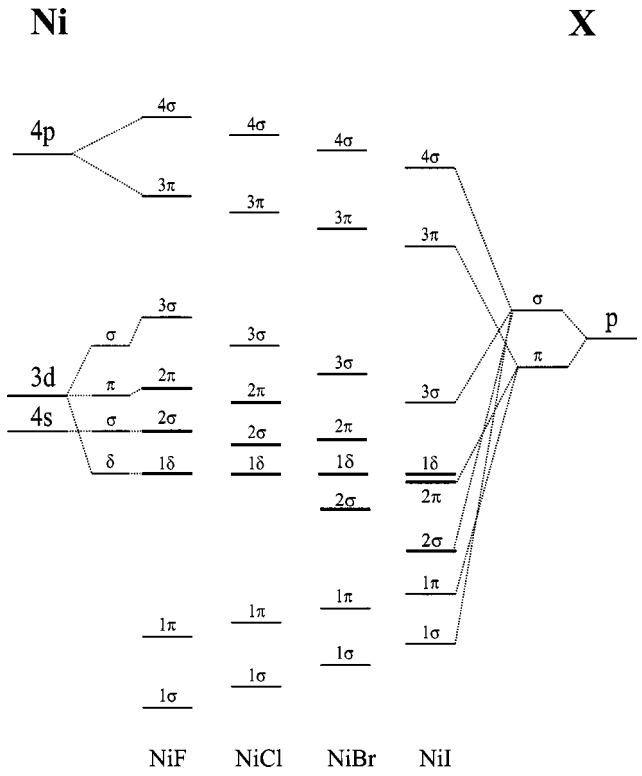

FIG. 4. Molecular orbital energy level diagram of nickel monohalides.

atoms indicates how easily the outermost electron can be removed, which establishes the relative energy of the valence orbitals of the Ni and halogen atoms. Figure 4 shows the MO formed from the Ni $4s$ and $3d$ atomic orbitals (AOs) and the iodine $5p$ AOs. The bonding orbitals 1σ and 1π are mainly formed from the iodine $5p\sigma$ AO with the Ni $4s\sigma$ AO and iodine $5p\pi$ AOs with Ni $4p\pi$ AOs, respectively. The 2σ MO is based on the combination of Ni $4s\sigma$ and the iodine $5p\sigma$ AOs. The 2π MO is formed from the Ni-based $3d\pi$-$4p\pi$ and of the iodine $5p\pi$ AOs. The 1δ MO is essentially a pure Ni $3d\delta$ AO because there is no other orbital of δ symmetry lying nearby. The electronic configurations giving rise to the observed ground and low-lying electronic states are

$$(2\sigma)^2(2\pi)^4(1\delta)^3 \quad X\,^2\Delta_i, \tag{2}$$

$$(2\sigma)^2(2\pi)^3(1\delta)^4 \quad A\,^2\Pi_i, \tag{3}$$

$$(2\sigma)^1(2\pi)^4(1\delta)^3(3\sigma)^1 \quad (2)\,^2\Delta_i,\,^4\Delta_i, \tag{4}$$

$$(2\sigma)^2(2\pi)^3(1\delta)^3(3\sigma)^1 \quad (2)\,^2\Pi_i,\,^4\Pi_i;(2)\,^2\Phi_i,\,^4\Phi_i. \tag{5}$$

The $[13.9]\ ^2\Pi_{3/2}-X\,^2\Delta_{5/2}$ and the $[14.6]\ ^2\Delta_{5/2}-X\,^2\Delta_{5/2}$ transitions observed in this work are likely to be the promotion of an electron, respectively, from the 2π MO and 2σ MO to the 3σ MO. The 1δ orbital is always with one vacancy to be filled, which gives rise to the observed inverted states. From the MO energy level diagram in Fig. 4, we could also explain the ionic nature of these monohalides. There are five valence electrons in the p orbitals of the halogen and ten valence electrons in the $3d$ and $4\,s$ orbitals of nickel. Since the 1σ and 1π MOs are essential the p AOs of the halogen atom, in order to probably fill up these two MOs: one electron from the valence shell of the Ni atom has to be transferred to the 1π orbital. Such a move of electron from the Ni atom to the halogen atom forms the expected Ni^+X^- ionic compound. The other nine electrons of the Ni atom occupy the 2σ, 2π, and 1δ MOs as shown in the above electronic configurations.

Generally, the electronic states of NiI should be quite similar to those found in isovalent molecules such as NiF, NiCl, and NiBr. These isovalent molecules all have $X\,^2\Pi_{3/2}$ ground state and the $A\,^2\Delta_{5/2}$ lying higher in energy, however, NiI has $X\,^2\Delta_{5/2}$ as its ground state that deserves some discussion because it is not the expected $X\,^2\Pi_{3/2}$ state as in NiF,[12] NiCl,[13] and NiBr.[24] Table IV lists the spectroscopic parameters for the low-lying $^2\Pi$ and $^2\Delta$ states observed for nickel monohalides. It is interesting to note the energy separation between the $A\,^2\Delta_{5/2}$ and $X\,^2\Pi_{3/2}$ drops from 830 cm^{-1} in NiF, 161 cm^{-1} in NiCl to 37.5 cm^{-1} in NiBr. Since the $A\,^2\Delta_{5/2}$ state arises from the unpaired electrons in the 1δ MO that is mainly coming from the nickel atom and subject to the least influence from any halogen atom, the relative drop in energy separation should be viewed as the decrease in energy that occur in the 2π and 2σ orbitals in the halides rather than the 1δ MO. Furthermore, the decrease in energy of the 2π and 2σ orbitals can be ascribed to the change in the relative orbital energy of the p AO of the halogens with respect to the $3d$ and $4s$ AO of Ni. From the trend observed in NiF, NiCl, and NiBr, it is plausible to explain that the decrease in energy of the 2σ and 2π MO with respect to the 1δ MO in NiI is the major reason for the $^2\Delta_{5/2}$ state as the ground state for NiI rather than the $^2\Pi_{3/2}$ state as in the other isovalent monohalides. Presently, we only know that the 1δ and 2π MOs are lying very close in energy to each other, but which MO is of lower energy is still a question; this is because the correlation energy of the electrons in each MO is not known. In order to better understand the whole picture, spin–orbit interaction should be considered. The work on NiF and NiCl as listed in Table IV provides information for us to analyze the spin–orbit interaction of the low-lying electronic states.[30] The following is a summary of the observed spin–orbit separations of NiF and NiCl (cm^{-1}):

Electronic state	Spin–orbit separation, $A\Lambda$		Spin–orbit constant, A	
	NiF	NiCl	NiF	NiCl
$X\,^2\Pi_{3/2}$		398		398
$A\,^2\Delta_{5/2}$	1394	1488	697	744

The spin–orbit separation of an electronic state in Hund's case (a) is given by $A\Lambda$, where A is the spin–orbit constant and Λ is the orbit angular momentum projected onto the intermolecular axis.[29] For the $^2\Pi$ and $^2\Delta$ states, the spin–orbit separation between the two Ω components are, respectively, A and $2A$.

The microscopic spin–orbit Hamiltonian[31] can be written as $H_{so}=\Sigma_i a_i l_i \cdot s_i$, which is a single-electron operator. Using this operator and a single configuration representation for the electronic state, it is possible to correlate the observed

TABLE IV. Spectroscopic constants for low-lying $^2\Pi$ and $^2\Delta$ states of nickel monohalides (cm^{-1}).

NiF		NiCl		NiBr[24]		NiI	
$X\ ^2\Pi_{3/2}$	$B_0=0.387\ 81$ (Ref. 12) $r_0(\text{Å})=1.7403$	$X\ ^2\Pi_{3/2}$	$B_0=0.181\ 50$ (Ref. 13) $r_0(\text{Å})=2.0637$ $\omega_e=425.63$	$X\ ^2\Pi_{3/2}$	$B_0=0.104\ 60$ $r_0(\text{Å})=2.1963$	$X\ ^2\Delta_{5/2}$	$B_0=0.076\ 86$ $r_0(\text{Å})=2.3479$
$A\ ^2\Delta_{5/2}$	$T_0=829.48$ (Ref. 12) $B_0=0.388\ 54$ $r_0(\text{Å})=1.7386$ $\omega_e=646\times10^7$	$A\ ^2\Delta_{5/2}$	$T_e=157.70$ (Ref. 13) $B_e=0.184\ 31$ $r_e(\text{Å})=2.0480$ $\omega_e=435.52$	$A\ ^2\Delta_{5/2}$	$T_0=37.46$ $B_0=0.107\ 71$ $r_0(\text{Å})=2.1644$	[13.9] $^2\Pi_{3/2}$	$T_e=13\ 761.28$ $B_e=0.068\ 40$ $r_e(\text{Å})=2.4834$ $\omega_e=235.09$
$A\ ^2\Delta_{3/2}$	$T_e=2223.56$ (Ref. 11) $B_0=0.388\ 35$ $r_0(\text{Å})=1.7390$	$X\ ^2\Pi_{1/2}$	$T_e=385.666$ (Ref. 30) $B_0=0.180\ 78$ $r_0(\text{Å})=2.0678$	[13.2] $^2\Pi_{3/2}$	$T_e=13\ 047.81$ $B_e=0.096\ 94$ $r_e(\text{Å})=2.3502$ $\omega_e=292.97$	[14.6] $^2\Delta_{5/2}$	$T_e=14\ 468.67$ $B_e=0.067\ 50$ $r_e(\text{Å})=2.5081$ $\omega_e=230.56$
[11.1] $^2\Pi_{3/2}$	$T_0=11\ 096.05$ (Ref. 12) $B_0=0.367\ 11$ $r_0(\text{Å})=1.7886$	$A\ ^2\Delta_{3/2}$	$T_0=1645.83$ (Ref. 15) $B_0=0.182\ 29$ $r_0(\text{Å})=2.0593$				
		[9.1] $^2\Pi_{3/2}$	$T_0=9101.261$ (Ref. 30) $B_0=0.171\ 773$ $r_0(\text{Å})=2.1214$				
		[13.0] $^2\Pi_{3/2}$	$T_0=12\ 959.25$ (Ref. 18) $B_0=0.167\ 69$ $r_0(\text{Å})=2.147$				

spin–orbit constant to the one electron spin–orbit parameter. For a $^2\Delta_{5/2}$ substrate in a δ^3 configuration, $|^2\Delta_{5/2},\delta^3\rangle$, the wave function is $|\delta^+\alpha\delta^+\beta\delta^-\alpha\rangle$, thus

$$\langle {}^2\Delta_{5/2},\delta^3|\mathbf{H_{so}}|{}^2\Delta_{5/2},\delta^3\rangle=\langle\delta^-\alpha|al_z\cdot s_z|\delta^-\alpha\rangle = -1/2a_\delta. \quad (6)$$

The contribution of the $\delta^+\alpha\delta^+\beta$ subshell to the spin–orbit matrix element is zero. For the $^2\Delta_{3/2}$ substate, the wave function is $|\delta^+\alpha\delta^+\beta\delta^-\beta\rangle$, and

$$\langle {}^2\Delta_{3/2},\delta^3|\mathbf{H_{so}}|{}^2\Delta_{3/2},\delta^3\rangle=\langle\delta^-\beta|al_z\cdot s_z|\delta^-\beta\rangle=1/2a_\delta, \quad (7)$$

therefore, the spin–orbit constant, A, for a $^2\Delta$ state in δ^3 configuration is related to a_δ,

$$A(^2\Delta_i,\delta^3)=-a_\delta. \quad (8)$$

Similarly, the spin–orbit constant for a $^2\Pi$ state in the π^3 configuration is related to a_π,

$$A(^2\Pi_i,\pi^3)=-a_\pi. \quad (9)$$

Since the spin–orbit interaction observed in the nickel monohalides is dominated by the Ni atom, the value of a_δ can be compared with the observed spin–orbit constant directly. The atomic spin–orbit parameter (ξ) is 672 cm^{-1} for Ni^+.[31] In the case of a $^2\Delta$ state mainly from Ni^+ $3d\delta$, $A=a_\delta=672\ cm^{-1}$. This a_δ value is in very good agreement with the observed spin–orbit constant of 697 and 744 cm^{-1} for NiF and NiCl, respectively. We do not have any theoretical estimate of the a_π value at the present moment. Nevertheless, when compared with the spin–orbit constant, $A=349\ cm^{-1}$, of the $^3\Pi$ state of NiO,[32] the agreement between the measured spin–orbit constant in the $^2\Pi$ state with $A=398\ cm^{-1}$ is excellent. This indicates that the Ni^+ atom also dominates the spin–orbit interaction in the Π state. Judging from the spin–orbit separation of the $^2\Delta_i$ state is four times larger than the $^2\Pi_i$ state and the tendency of the 2π MO is moving closer to the 1 δ MO, it is legitimate to expect the $^2\Delta_{5/2}$ to be the ground state of NiI. The theoretician performing *ab initio* calculations incorporating a spin–orbit interaction could help to compute the energy of the low-lying spin–orbit components of these states. Furthermore, we have work in progress to search for the $A\ ^2\Pi_{3/2}$ state that is predicted to lie not too far from the $X\ ^2\Delta_{5/2}$ in NiI.

It is also interesting to note the variations of spectroscopic properties down the halogen group among the ground and low-lying states. The bond length of the electronic states increases down the group is due to the increase in the size of the atom down the group. The bond length of the $A\ ^2\Delta_{5/2}$ state arises from electronic configuration (2) in NiF, NiCl, and NiBr is always shorter than that of the $X\ ^2\Pi_{3/2}$ from electronic configuration (3), which is consistent with the bonding nature of the 2π MO and the nonbonding nature of the 1δ MO. The vibrational constant of the nickel monohalides decreases down the halogen group. Since the force constant is proportional to the product of the reduced mass and the square of the vibrational frequency, we note that the force constant also decreases down the group, which indicates that the chemical bond between the metal and the halides weaken from F to I. This is expected as the order of the halogen ion in the spectrochemical series is $F^->Cl^->Br^->I^-$.

ACKNOWLEDGMENTS

The work described here was supported by grants from the Committee on Research and the Conference Grants and

the Hung Hing Ying Physical Sciences Research Fund of the University of Hong Kong. We thank Mr. P. M. Yeung for providing technical help.

[1] S. R. Langhoff and C. W. Bauschlicher, Jr., Annu. Rev. Phys. Chem. **39**, 181 (1988).
[2] C. Dufour, P. Carette, and B. Pinchemel, J. Mol. Spectrosc. **148**, 303 (1991).
[3] C. Dufour, I. Hikmet, and B. Pinchemel, J. Mol. Spectrosc. **158**, 392 (1993).
[4] C. Dufour, I. Hikmet, and B. Pinchemel, J. Mol. Spectrosc. **165**, 477 (1994).
[5] A. Bouddou, C. Dufour, and B. Pinchemel, J. Mol. Spectrosc. **168**, 477 (1994).
[6] C. Dufour and B. Princhemel, J. Mol. Spectrosc. **173**, 70 (1995).
[7] C. Focsa, C. Dufour, and B. Pinchemel, J. Mol. Spectrosc. **182**, 65 (1997).
[8] Y. Chen, J. Jin, C. Hu, X. Yang, X. Ma, and C. Chen, J. Mol. Spectrosc. **203**, 37 (2000).
[9] J. Jin, Y. Chen, X. Yang, Q. Ran, and C. Chen, J. Mol. Spectrosc. **208**, 18 (2001).
[10] J. Jin, Q. Ran, X. Yang, Y. Chen, and C. Chen, J. Phys. Chem. A **105**, 11177 (2001).
[11] Y. Krouti, T. Hirao, C. Dufour, A. Boulezhar, B. Pinchemel, and P. F. Bernath, J. Mol. Spectrosc. **214**, 152 (2002).
[12] B. Pinchemel, T. Hirao, and P. F. Bernath, J. Mol. Spectrosc. **215**, 262 (2002).
[13] T. Hirao, C. Dufour, B. Pinchemel, and P. F. Bernath, J. Mol. Spectrosc. **202**, 53 (2000).
[14] A. Poclet, Y. Krouti, T. Hirao, B. Pinchemel, and P. F. Bernath, J. Mol. Spectrosc. **204**, 125 (2000).
[15] Y. Krouti, A. Poclet, T. Hirao, B. Pinchemel, and P. F. Bernath, J. Mol. Spectrosc. **210**, 41 (2001).
[16] E. Yamazaki, T. Okabayashi, and M. Tanimoto, Astrophys. J. Lett. **551**, L199 (2001).
[17] L. C. O'Brien, K. M. Homann, T. L. Kellerman, and J. J. O'Brien, J. Mol. Spectrosc. **211**, 93 (2001).
[18] J. J. O'Brien, J. S. Miller, and L. C. O'Brien, J. Mol. Spectrosc. **211**, 93 (2002).
[19] C. A. Rice and L. C. O'Brien, J. Mol. Spectrosc. (in press).
[20] A. B. Darji and N. R. Shah, Curr. Sci. **48**, 349 (1979).
[21] R. Gopal and M. M. Joshi, Curr. Sci. **50**, 1061 (1981).
[22] R. Gopal and M. M. Joshi, Indian J. Phys., B **59**, 309 (1985).
[23] S. P. Reedy, N. Narayana, and P. T. Rao, Opt. Pura Apl. **20**, 69 (1987).
[24] J. W.-H. Leung, X. Wang, and A. S.-C. Cheung, J. Chem. Phys. **117**, 3694 (2002).
[25] Q. Ran, W. S. Tam, C. Ma, and A. S.-C. Cheung, J. Mol. Spectrosc. **198**, 175 (1999).
[26] J. W.-H. Leung, F. C.-Y. Hung, and A. S.-C. Cheung, Chem. Phys. Lett. **363**, 117 (2002).
[27] S. Gerstenkorn and P. Luc, *Atlas der Spectra d'absorption de la Molecule d'iode* (Editions du CNRS, Paris, 1978); S. Gerstenkorn and P. Luc, Rev. Phys. Appl. **14**, 791 (1979).
[28] See EPAPS Document No. E-JCPSA6-119-009347 for the observed line positions of the $[13.9]^2\Pi_{3/2}-X\,^2\Delta_{5/2}$ and $[14.6]^2\Delta_{5/2}-X\,^2\Delta_{5/2}$ systems of NiI. A direct link to this document may be found in the online article's HTML reference section. The document may also be reached via the EPAPS homepage (http://www.aip.org/pubservs/epaps.html) or from ftp.aip.org in the directory /epaps/. See the EPAPS homepage for more information.
[29] G. Herzberg, *Spectra of Diatomic Molecules* (van Nostrand, New York, 1950).
[30] L. C. O'Brien and S. Tumturk, International Symposium on Molecular Spectroscopy, Ohio State University, Columbus, OH, June, 2003, Paper MB08.
[31] H. Lefebvre-Brion and R. W. Field, *Perturbations in the Spectra of Diatomic Molecules* (Academic, New York, 1986).
[32] E. J. Friedman-Hill and R. W. Field, J. Mol. Spectrosc. **155**, 259 (1992).